Thermal stability and hydrogenation behavior of Zr–1Nb alloy with TiN_x and Ti/TiN_x coatings

E B Kashkarov[1], **O V Vilkhivskaya**[2], **S A Zakharchenko**[1]
[1]General Physics Department, Tomsk Polytechnic University, Tomsk 634050, Russia
[2]Department of Atomic Energy Safety, Troitsk Institute for Innovation and Fusion Research, Moscow, Troitsk 142190, Russia

Abstract. Titanium nitride coatings were deposited by reactive dc magnetron sputtering (dcMS) to protect Zr–1Nb alloys from hydrogen embrittlement. Dense titanium (Ti) interlayer was prepared between TiN_x protection film and a Zr substrate to improve thermal stability and adhesion between the TiN_x and the substrate at high temperatures. Hydrogen absorption of Zr–1Nb with TiN_x and Ti/TiN_x at 623 K was reduced in comparison with uncoated Zr–1Nb. No peeling or cracks of Ti/TiN_x coatings is observed after thermal cycling up to 1073 K. The high temperature (1073 K) hydrogenation behaviour differs from the hydrogenation at lower temperature by increasing the amount of dissolved hydrogen in the β-phase of zirconium. The higher rate of hydrogen absorption by Zr–1Nb with TiN_x was observed due to the coating delamination as a result of differences in thermal expansion coefficients, while Ti/TiN_x demonstrates the lower hydrogen absorption at 1073 K and good adhesion strength.

1. Introduction

Hypothetical nuclear accidents can create real danger to the zirconium alloys and stability of parts made of these alloys, especially such as loss of coolant accident (LOCA) and reactivity initiated accidents (RIA). Hydrogen degradation can manifest itself in appearance of hydride phases resulting in substantial loss of plasticity, increase in ductile-brittle transition, and sometimes in decrease in mechanical strength [1–3]. In Russian Water-Water Energetic Reactor (WWER) and High Power Channel Reactor (RBMK) the Zr–1Nb alloy is used as cladding material. Rapid changes in cladding temperature and increase in the hydrogen absorption rate are the results of LOCA and RIA accidents. The magnetron sputtering and vacuum arc deposition are the main methods used for more than 60 years in various industries for coating deposition and surface modification of structural materials [4–6]. The main advantage of the VAD method is the higher degree of ionization and the higher energy of deposited particles, which increases the density and adhesion of coating by generating of the mixing zone contained deposited and substrate materials. Titanium nitride (TiN) deposited by magnetron sputtering and vacuum arc deposition is promising in protection of zirconium alloys from hydrogen embrittlement [7–9]. Furthermore, TiN coatings have excellent erosion resistance, which favourably affects the fretting resistance of the coatings. The differences between the temperature expansion coefficient of the TiN coating and zirconium alloy lead to the coating degradation. It is known that the coatings obtained by dcMS have low adhesion strength in comparison with FVAD coatings. Moreover, the titanium thermal expansion coefficient of 8.6×10^{-6} K^{-1} is in the range between zirconium (5.7×10^{-6} K^{-1}) and titanium nitride (9.35×10^{-6} K^{-1}). It suggests that it will sustain the balancing thermal expansion coefficient between the substrate and the coating and improve the adhesion strength. In this work, we investigate the operational stability characteristics of

hydrogen-impermeable TiN and Ti/TiN protective coatings deposited on Zr–1Nb substrates by dcMS and FVAD/ dcMS methods under high-temperature hydrogenation and thermocycling conditions.

2. Experimental procedure

2.1 Coating Deposition

The Zr–1Nb alloy samples with fixed size of 0.5 mm in thickness and 20 mm in diameter were previously polished using sandpaper to the roughness of 0.1 μm. Initially, the samples were rinsed with alcohol and put into vacuum chamber. Then, the samples were subjected to ion bombardment in argon glow discharge to clean the surface from oxides and organic contamination at 1500 V for 5 min. Finally, TiN and Ti/TiN coatings were deposited onto Zr–1Nb substrates by dcMS and FVAD/dcMS methods, respectively. For magnetron sputtering, high-purity Ti target (99.99%) with dimensions of 100×8 mm was used. TiN coatings were deposited for 30 min by reactive sputtering with the flow rates ratio of $Q_{Ar}/Q_{N2}=4/3$ at the constant pressure 0.15 Pa, target power 2.6 kW and current 4 A. The distance between the target and the samples was 150 mm. For FVAD – the cathodic vacuum arc evaporation system equipped with coaxial plasma filter [10] was used. Process parameters for FVAD of Ti (99.8 % purity) interlayer are: 0.2 Pa total pressure, 110 A arc current, 150 V negative pulsed substrate bias with 100 kHz pulse repetition frequency, 5 μs pulse length and 3 A peak pulse current.

2.2. Hydrogenation and Thermal Cycling

Hydrogenation of the samples was performed from hydrogen atmosphere on the automated complex Gas Reaction Controller (USA) at 623 K and 1073 K temperatures for 60 min. The heating rate and hydrogen pressure in the chamber was 6 K/min and 2 atm, respectively. The hydrogenation temperatures were chosen to simulate the working temperature of zirconium fuel cladding during stationary operation and in LOCA transient temperature conditions in the nuclear reactor core.

Thermal cycling of the samples was performed with the water cooled vacuum furnace. The residual pressure in the chamber was $(6–7)\times10^{-3}$ Pa. Heating and cooling rates were 200 and ~ 2000 K/min, respectively. Three cycles of heating and cooling the Zr–1Nb specimens coated with TiN and Ti/TiN were performed.

2.3. Characterization

The morphology of the coatings was studied using scanning electron microscope (Hitachi TM-3000, Japan). The phase identification and structural investigations of the deposited coatings were performed by X-ray diffraction with CuK_α radiation (1.5410 Å wavelength) using Shimadzu XRD-7000 (Japan) diffractometer in asymmetric mode at 40 kV, 30 mA and θ=3° fixed angle. The film thickness was measured by simple ball-cratering method performed with Calotest CAT-S. The measurement of adhesion strength was performed with MicroScratchTester MST-S-AX technique by scratch method using a diamond indenter. Scratching parameters are 0.01 N initial load, 20 N final load, 9.63 mm/min scratching speed and 10 mm scratch length.

3. Results and discussion

Figure 1 shows that deposited TiN_x coating has a cubic NaCl-type structure. It can be seen that the orientation in the plane (200) is the reflection of major intensity and it remains as the most intense for both TiN_x and Ti/TiN_x coatings. Similar results in preferred TiN orientation in plane (200) have also been observed in the report [11]. The less intensive (220) and (222) reflections have been observed. The reflections in plane (111) are difficult to resolve due to the merger with substrate (Zr) reflections. Ti interlayer is formed after vacuum arc deposition.

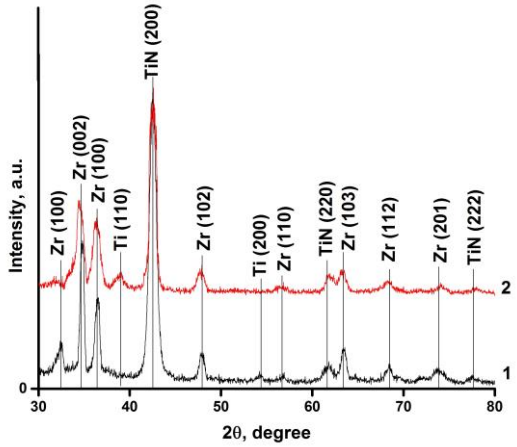

Figure 1. XRD pattern of Zr–1Nb with TiN_x (1) and Ti/TiN (2)

Figure 2 compares samples states after hydrogenation from hydrogen atmosphere at 623 K for an elongated period of time to the point where the initial Zr–1Nb specimen cracks up to pieces, while the specimen with TiN_x coating retains its shape. Surely, at the operational (normal) conditions of the reactor core, primary circuit coolant (for instance, for H_2O in WWER-1000: temperature ~600 K and pressure of 16 MPa) hydrogen absorption rate is not that intensive. At high burnups (>50 MW·days/kgU), developing of hydrides of mainly tangential orientation contains fraction of hydrogen that does not exceed 0.01 % [12].

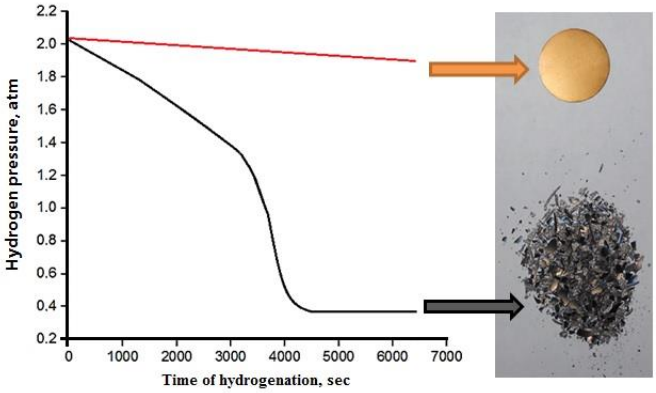

Figure 2. Hydrogen absorption curve for the initial (bottom) and coated with TiN_x (top) samples at 623 K for 2 hours

Figure 3 shows SEM surface morphologies of both TiN_x and Ti/TiN_x coatings before and after thermal cycling up to 1073 K (three cycles). The sputtered TiN_x coating shows excessive surface roughness and traces of grinding (Figure 3). After thermal cycling, the surface of the sample with TiN_x contained peeling of the coating and cracks formed during thermal expansion (Figure 3a and 3b), which was not observed in the sample with a Ti/TiN_x coating (Figure 3c and 3d).

The deposition of TiN_x coating reduces hydrogenation of Zr–1Nb alloy at 623 K. The sufficient reduction of the hydrogen absorption was observed for 1.5 μm TiN_x coating, while the thickness of coating was measured by ball-cratering method. However, the formation of cracks and peelings of coating after thermal cycling up to 1073 K has a strongly negative effect on hydrogenation behaviour and protective properties of the coating.

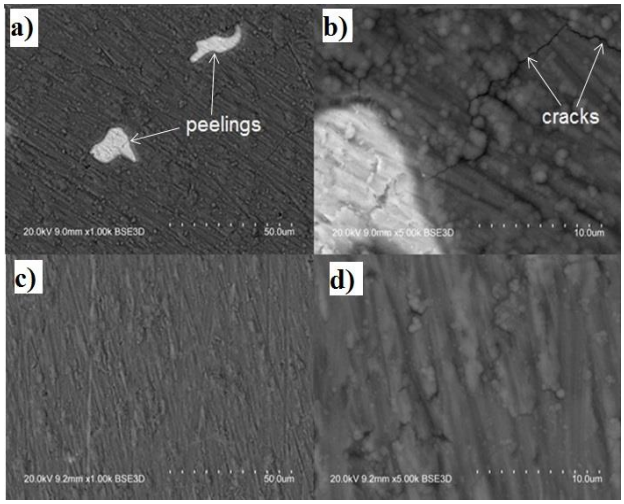

Figure 3. SEM images of TiN (a, b) and Ti/TiN (c, d) after thermal cycling up to 1073 K

The hydrogen absorption rate of Ti/TiN_x is on the same level with TiN_x without interlayer during hydrogenation at 623 K (Figure 4a). However, hydrogenation behavior at the temperature of 1073 K significantly differs for all the samples. The thermal solubility of hydrogen in α-Zr is very low, it is equal to ~ 6 at. % at a temperature of eutectoid transformation (820 K) and decreases rapidly with temperature. Nevertheless, the high-temperature β-Zr (bcc) dissolves up to ~ 50 at. % of hydrogen. Hydrogen is a very strong β-stabilizing element – with increasing hydrogen content the temperature of α→β transformation decreases from 1136 K for undoped Zr to ~ 820 K at a hydrogen concentration of ~ 6 at. % [13]. At room temperature, the thermal solubility of α-Zr hydrogen solubility is less than 1 ppm. Thus, only a small amount of hydrogen in the lattice of α-Zr can be dissolved, which causes the rapid precipitation of hydrides that increases hydrogen absorption rate of the initial sample by the cracking of hydrides. Nevertheless, the samples coated with TiN_x and Ti/TiN_x accumulate a small amount of hydrogen for 1-hour hydrogenation, which explains the linear dependence of hydrogen absorption determined by a diffusion barrier of titanium nitride coating. Hydrogen saturation of Zr–1Nb at 1073 K leads to the phase transformation (α+β)→β with increasing hydrogen content. In this case, hydrogen dissolves in the β-phase and the hydrogen absorption curve becomes saturated gradually when the concentration of hydrogen is determined by Sievert law. At high temperatures, zirconium hydride decomposes and does not transform the dissolved hydrogen in the bound state. The hydrogen absorption at 1073 K is also reduced for the coated with TiN_x and Ti/TiN_x samples. However, we can observe a higher rate of hydrogen absorption by Zr–1Nb with TiN_x due to the coating delamination as a result of differences in thermal expansion coefficients.

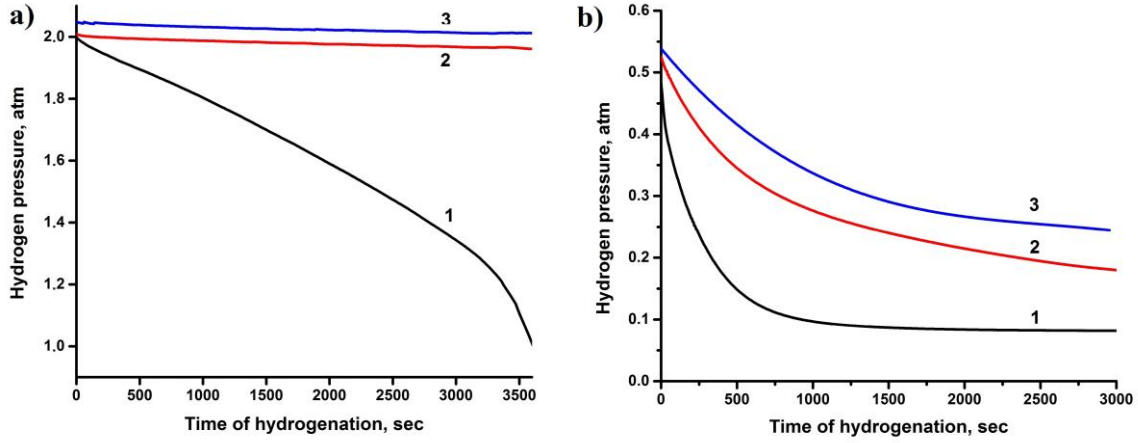

Figure 4. Hydrogen absorption curve at 623 K (a) and 1073 K (b) for: 1 – initial Zr–1Nb, 2 – Zr–1Nb with TiN_x, 3 – Zr–1Nb with Ti/TiN_x

The adhesion strength of TiN_x and Ti/TiN_x coatings was measured by scratch method. Typycal SEM image of the scratch after thermal cycling is shown in Figure 5, where coatings retained on the substrate up to 8 N normal load applied to indenter. This result demonstrates that Ti/TiN_x coating retains the adhesion properties when exposed to rapidly changing temperatures in the range of 293-1073 K.

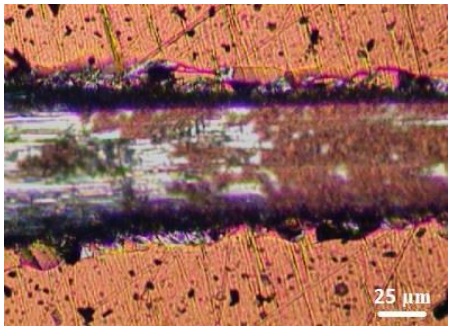

Figure 5. Typical SEM image of scratch for Ti/TiN_x coating on Zr–1Nb substrate

4. Conclusion

TiN_x and Ti/TiN_x coatings were deposited onto Zr–1Nb by dcMS and combination of FVAD and dcMS methods, respectively. TiN_x coating significantly reduces hydrogen absorption of Zr–1Nb alloy. The cracking of TiN_x coating was observed after thermal cycling up to 1073 K. Nevertheless, Ti/TiN_x coatings are resistant during thermal cycling in the temperature range of 293–1073 K, which is associated with the balancing of thermal expansion coefficient between Zr–1Nb and TiN_x coating. The hydrogen sorption rate of Ti/TiN_x remains at the same level with TiN_x during hydrogenation at 623 K. The hydrogenation behaviour of Zr–1Nb significantly differs at 1073 K for Ti/TiN_x and TiN_x coatings; the latter has a higher rate of hydrogen absorption.

Acknowledgment

The reported study was funded by RFBR according to the research project No. 16-38-00709 and "UMNIK" program by Fund of assistance to development of small forms of the enterprises in the scientific and technical sphere.

References

[1] Chernyaeva T P, Ostapov A V 2013 *Problems of Atomic Science and Technology* **87** 16–31.
[2] Kashkarov E B, Nikitenkov N N, Syrtanov M S, Sutygina A N, Shulepov I A, Lider A M 2016 *Appl. Surf. Sci.* **370** (2016) 142–148.
[3] Zielinski A, Sobieszczyk S 2011 *Int. J. Hydrogen Energy* **36** 8619–8629.
[4] Kelly P J, Arnell R D 2000 *Vacuum* **56** 159–172.
[5] Sidelev D V, Yurjev Y N 2014 *Advanced Materials Research* **1040** 748–752.
[6] Anders A 2014 *Proc. Int. Symp. on Discharges and Electrical Insulation in Vacuum*, ISDEIV 201–204.
[7] Kashkarov E B, Nikitenkov N N, Tyurin Yu I, Syrtanov M S, Zhang L 2015 *IOP Conf. Ser.: Mater. Sci. Eng.* **81** (1) 012017.
[8] S.V. Ivanova E M, Glagovskiy I A, Khazov et al. 2008 *Proc. IV Int. Conf. on Interaction of Hydrogen Isotopes with Structural Materials* 51–75.
[9] Kim I, Khatkhatay F et al. 2012 *J. Nucl. Mater.* **429** 143–148.
[10] Ryabchikov A I and Stepanov I B 2009 *Surface and Coating Technology* **203** 2784.
[11] Dupin N, Ansara I, Servant C, Toffolon C, Lemaignan C, Brachet J C 1999 *J. Nucl. Mater.* **275** (3) 287–295.
[12] Markov D V et al, State of fuel rods spent in the VVER-1000 reactor up to a fuel burnup of 75 MWdays/kgU, JSC "SSC RIAR", IAEA, NCL Collection Store.
[13] Hong E, Dunand D C, Choe H 2010 *Int. J. Hydrogen Energy* **35** (11) 5708–5713.